Mixotrophy for carbon-conserving waste upcycling

Michael Weldon[1] & Christian Euler[1,*]

[1] Department of Chemical Engineering, University of Waterloo

[*] to whom correspondence should be addressed, ceuler@uwaterloo.ca

Abstract

Modern chemical production, on which human quality of life depends, is unsustainable. Alternative, sustainable manufacturing routes must therefore be developed. Electrochemical and biological processes offer promise for upgrading waste streams, including recalcitrant CO_2 and plastic-derived wastes. However, these processes are challenged by the inherent heterogeneity and high energy input requirements for upcycling of the chemical endpoints of the "take-make-waste" economy. *Cupriavidus necator* is emerging as a potentially useful catalyst to valorize such complex feedstocks because of its extreme metabolic flexibility, which allows it to utilize a wide array of substrates, and its ability to use CO_2 directly via the Calvin-Benson-Bassham cycle. *C. necator* natively oxidizes hydrogen to power carbon utilization, but its inherent flexibility offers an as-yet unexplored opportunity to couple waste stream oxidation with CO_2 utilization instead, potentially enabling carbon conservative waste upcycling. Here, we uncover the constraints on carbon conservative chemical transformation using *C. necator* as a model. We systematically examine the carbon yield and thermodynamic feasibility of mixotrophic scenarios that combine waste-derived carbon sources with hydrogen oxidation to power carbon reassimilation. Then, we evaluate carbon-carbon mixotrophic scenarios, with one carbon source providing electrons in place of hydrogen oxidation. We show that acetate, ethylene glycol, and glycerol all have high potential as inputs to carbon-neutral or carbon-negative mixotrophic fermentative upgrading, with acetate being critical to all scenarios explored here. In contrast, we find that carbon conservation is likely infeasible for most other waste-derived carbon sources. This work provides a roadmap to establishing novel *C. necator* strains capable of carbon efficient waste upcycling.

CO_2 reduction | metabolism | constraint-based analysis | pathway engineering

Introduction

Today, chemical production is heavily reliant on petroleum: thousands of chemical products begin as petroleum, and much of the energy used to produce them is also petroleum-derived [1, 2]. Continued long-term reliance on this carbon source is impossible because its accessible reserves are predicted to run out before the end of the century [3, 4]. CO_2 is an attractive replacement because it can be sustainably sourced as part of the global carbon cycle and its ubiquity as a product of human industrial activities could make its use cost-effective. To date, the primary strategies for CO_2 upgrading have been electrochemical and biological.

In electrochemical reduction of CO_2 (eCO_2R), electrical energy is used to convert CO_2 and a hydrogen/electron donor - water or H_2 - into value-added chemicals. The sustainability of such electroreduction processes depends on the sustainability of the energy generation methods used to power them [5]. Power grids are unlikely to be able to quickly accommodate the energy demands of large-scale chemical production via eCO_2R without support from the continued burning of fossil fuels for electricity generation [6]. Broad adoption of CO_2 upgrading will therefore require massive expansion of renewable energy generation alongside efficiency improvements to existing renewable energy technologies [6, 7].

In addition to these significant energy requirements, eCO_2R also requires a large volume supply of hydrogen that must also be sourced sustainably. Green hydrogen is often considered as a viable way to meet this demand, but the required technology for its production has not been demonstrated at an industrial scale to date [8, 9]. It will thus be a significant challenge to meet the 250 Mt green hydrogen demand that is predicted by 2050. At this scale, the generation of this input stream alone would use up approximately 90% of the energy budget of the chemical sector.

Moreover, increasingly limited water supplies in a changing climate will likely set an upper bound on green hydrogen production capacity [9]. The constraints on sustainable hydrogen production therefore represent a significant barrier to the expansion of eCO_2R-based chemical production [7].

Even if these material and energetic barriers are overcome, the scope of products accessible via eCO_2R will have to be expanded for it to be a meaningful approach to meet the current chemical product needs of society. The primary outputs of eCO_2R processes to date have been C1 and C2, and to a lesser extent, C3 chemicals. Carbon monoxide, formic acid, ethylene, methanol, ethanol, methane, and *n*-propanol [10] are the most often reported products. Other C3 chemicals and some C4 chemicals have been observed in eCO_2R processes but at limited production rates and scales [11–13]. Part of the limitation of producing longer carbon chain molecules is that the C1/C2 intermediates are released from the catalyst before they can be extended [13]. As such, producing polymers and liquid fuels from CO_2 remains challenging, though work toward achieving sustainable conversion processes is accelerating [14, 15].

In contrast to electrochemical production methods, biological routes leverage the native ability of certain microbes to fix CO_2 as a way to produce value-added compounds. For example, acetone and isopropanol (C3 compounds) production by engineered *Clostridium autoethanogenum* grown on waste gas feedstocks ($CO_2/CO/H_2$) has been demonstrated at industrial scale with productivities reaching approximately 3 g/L/h and selectivities of up to 90% [16]. Anaerobic acetogens, such as *C. autoethanogenum*, are attractive for CO_2 utilization because they make use of the energy efficient Wood Ljungdhal pathway [17, 18] and do not require intensive process development for light delivery, as is the case with photosynthetic organisms [19, 20]. However, the strict anaerobic requirements of acetogens might limit the scope of products that is accessible via processes utilizing them in two ways. First, it stoichiometrically constrains oxygen availability, because oxygen can only come from the CO_2/CO feedstock in such processes. Second, it constrains the amount of energy available for the oxidation half of redox reactions, which puts an upper bound on the rate of CO_2 reduction.

The emerging industrial platform organism *Cupriavidus necator* can instead fix CO_2 in the presence of oxygen using a Calvin-Benson-Bassham (CBB) cycle powered by unique, oxygen-tolerant hydrogenases [21, 22]. *C. necator* has been used to produce a wide range of compounds, such as alcohols, fatty acids, terpenes, alkanes/alkenes, and organic acids [23]. Its ability to grow in the presence of oxygen, coupled with its inherent metabolic flexibility, makes it attractive as a host to oxidize alternative, non-sugar carbon sources, such as those derived from waste [24]. Furthermore, its ability to fix carbon in the presence of oxygen presents a significant opportunity to engineer the energetic coupling between oxidation pathways and CO_2 reduction. For example, the oxidation of reduced C1 substrates such as formate or methanol could provide energy in addition to that available from H_2 to drive CO_2 fixation. These two reduced feedstocks are currently accessible via eCO_2R, so may be made sustainably in the future. However, there are a number of other waste products that could potentially be used as sources of electrons to power CO_2 fixation in *C. necator*. Plastic monomers are of particular interest, because of the accelerating plastic crisis [25] and because *C. necator* natively produces polyhydroxybutyrate (PHB), a biopolymer that could be used as an alternative to petroleum-based plastics [26].

The idea of using mixotrophic approaches to increase carbon yield in microbial metabolism is not new, but has not been explored extensively or systematically. Previous *in silico* work evaluated mixotrophic strategies combining methanol oxidation with the transformation of various sugars via non-oxidative glycolysis (NOG). This demonstrated that methanol oxidation can increase the thermodynamic driving force for the production of desired chemicals, while conserving carbon [27]. Anaerobic carbon-conserving mixotrophy has been experimentally established in *C. autoethanogenum* engineered to utilize sugars and CO_2 [28] and *Clostridium carboxidivorans* engineered to use sugars and CO [29]. In both cases, yields were increased because reducing equivalents from sugar oxidation could be used to drive C1 reduction. More broadly, recent work has introduced the idea of rewiring metabolism to couple fermentative and respiratory pathways, with successful experimental implementation in an obligate anaerobic *Escherichia coli* strain and demonstration of carbon conservation [30]. In another instance, sugar-formate mixotrophy was achieved in *Yarrowia lipolytica*, with metabolically-derived CO_2 being electroreduced and fed back into the fermentation as formate to conserve carbon [31]. Similarly, there are some examples of successful direct, potentially mixotrophic, microbial transformation of the mixed outputs of eCO_2R cells [32], but with limited characterization of the mechanisms involved. Together, these examples demonstrate the validity and potential of mixotrophic use of CO_2-derived feedstocks to reduce the carbon intensity of fermentation.

Motivated by this previous work, and by the unique potential offered by the native ability of *C. necator* to fix carbon aerobically, we establish an *in silico* workflow here to systematically evaluate the stoichiometric and

thermodynamic constraints on mixotrophic scenarios making use of waste-derived, chemically reduced inputs. We initially consider co-consumption of carbon feedstocks which could be derived from waste streams with hydrogen as an electron donor. Then, we consider carbon-carbon mixotrophies in various configurations to uncover feasible, carbon-conserving routes to polymer and acid production that do not rely on hydrogen-derived electrons. We show that such mixotrophies are thermodynamically favourable, providing a route to the design of novel microbial systems capable of efficiently upcycling waste-derived feedstocks.

Results

Transformation of CO_2 to value-added products is a net chemical reduction process; therefore, it must be coupled to a complementary oxidation process. Based on the native ability of *C. necator* to couple hydrogen oxidation with CO_2 reduction, we aimed to evaluate the feasibility of coupling the oxidation of reduced, waste-derived carbon sources with CO_2 reduction instead (Fig. 1A), supposing that such coupling could decrease or eliminate the need for electrons from H_2. We considered reduced carbon sources available via three streams: plastic degradation and/or depolymerization; existing eCO_2R processes; and byproducts of bioprocesses. We further limited our search to carbon sources with known assimilation pathways, whether native to *C. necator* or not.

This yielded a list of nine possible substrates: formate, succinate, acetate, adipate, glycerol, ethylene glycol (EG), 1,4-butanediol (14BDO), ethanol (EtOH), and methanol (MeOH). Possible sustainable sources of these substrates, along with their assimilation pathways, are presented in Table 1. EG is unique among the substrates we considered in that it could be derived from all three streams considered. We also included CO_2 and fructose as benchmark carbon sources for comparison, since these are native substrates for *C. necator*. We added reported assimilation pathways for each of these carbon sources individually to a core model of *C. necator* metabolism [33] modified to include hydrogen oxidation (Fig 1B) to yield ten models capable of consuming non-CO_2 carbon sources plus one which can only use CO_2/H_2. For details about the core metabolic model, including modification and validation, see Materials and Methods.

Highly reduced substrates require less hydrogen for complete carbon conversion

Our focus was on the feasibility of various input scenarios, so we used PHB as a common product for comparison across the substrates evaluated here. PHB production envelopes for all models with complete reassimilation of carbon supported by H_2-derived electrons ('w/Reassim.') and without forced reassimilation ('w/out Reassim.'), generated using parsimonious FBA (pFBA) are plotted in Fig. S1B. In the reassimilation case, RuBisCO flux was allowed and H_2 uptake flux was unconstrained, while CO_2 flux was constrained to be zero. In the no reassimilation case, reassimilation was blocked by setting H_2 uptake to zero and allowing unconstrained exchange of CO_2. The production envelopes show that, unsurprisingly, complete carbon conservation supported by H_2 oxidation improves both biomass and PHB yield for all operating points relative to the case with no reassimilation.

Moreover, complete reassimilation removes constraints for all C2+ carbon sources and enables stoichiometric conversion to biomass and/or PHB for all carbon sources. As a result, production envelopes for the H_2-supported reassimilation case are defined solely by the carbon number of the substrate, as shown in Fig. 1D. In contrast, when some reassimilation is forced with H_2 uptake blocked - i.e. with all reducing equivalents derived from the carbon source alone - biomass and PHB yield are either not improved or are reduced (Fig S1A). This may help to explain why reassimilation is not observed to a significant degree in *C. necator* cells grown on fructose or succinate without H_2 [34], even though those cells express the enzymes required for assimilation [35].

H_2-supported complete reassimilation is driven by a mixture of reducing equivalents derived from the carbon source and H_2 (Fig 1A), so we expected that carbon sources with a high degree of reduction (DOR) would require less H_2 for complete reassimilation. Higher DOR means more electrons per carbon atom to produce the necessary reducing equivalents for CO_2 reassimilation. In Fig. 1C, the H_2 cost of reassimilating a single CO_2 molecule is presented for both growth-only and production-only extremes. The assimilation cost in the growth mode is variable across carbon sources, with no obvious correlation with DOR. This reflects the fact that conversion of each substrate to biomass requires substrate-specific pathways, each with their own redox efficiency. Substrates with higher H_2 required per CO_2 assimilated are converted to biomass with lower redox efficiency, because they require more additional reducing equivalents than those with lower H_2 costs.

For the production mode, there is a clear negative correlation between H_2 cost and DOR, as is apparent in Fig. 1E. The line in this figure shows the cost of assimilation in the case of full oxidation to CO_2, followed by reduction to PHB. Substrates above this line require more H_2 for CO_2-free PHB production than if they were completely oxidized to CO_2 first, while substrates below it require less hydrogen than this. The former might be more efficiently upcycled via a complete oxidation pathway, if one exists, coupled to reassimilation. The latter may be good targets for CO_2-free transformation to PHB using H_2 mixotrophy directly. Of the carbon sources investigated here, only glycerol and 14BDO fall below the line. This suggests that metabolic rewiring that accounts for redox efficiency may yield more carbon-efficient transformation pathways of many carbon sources. As an example, the redox efficiency of fructose utilization might be improved via application of the NOG pathway [27].

In the case of acetate and ethanol, CO_2 reassimilation is not required to produce PHB, since these substrates enter metabolism via acetyl-CoA, which is the starting point of the PHB pathway (Fig. 2C). This pathway requires reducing equivalents (Fig. 1A) that the conversion of acetate to acetyl-CoA does not provide, so CO_2-free acetate conversion requires electrons from H_2. However, the proximity of acetate to acetyl-CoA renders the H_2 cost per mole of substrate the second lowest among the carbon sources examined. CO_2-free conversion of ethanol requires no H_2 (Fig. 1C), because its oxidation to acetyl-CoA yields more reducing equivalents per carbon atom than are required to assimilate these carbon atoms. Thus, from a purely stoichiometric perspective, ethanol and acetate are ideal sole carbon sources for sustainable, CO_2-free PHB production.

These results suggest that if the native metabolic machinery of *C. necator* could be repurposed to reassimilate carbon generated in waste stream upcycling pathways, then higher biomass and product yields could be achieved relative to net CO_2-producing pathways. However, *C. necator* has been observed to natively reassimilate carbon only in marginal, nutrient-limited, and transitional situations [36]. Moreover, it has been shown that reassimilation offers no fitness benefit to *C. necator* grown on fructose or succinate, at least in the absence of H_2 [34]. Based on this empirical evidence, it is not clear that carbon reassimilation is feasible, even if it would increase yield.

CO_2-free fermentation via hydrogen mixotrophy has limited feasibility

We evaluated the thermodynamic feasibility of H_2-supported complete reassimilation for each carbon source by finding the associated max-min driving forces (MDF), and comparing those against the same for the non-reassimilation case. The MDF is the largest possible thermodynamic bottleneck for a given flux distribution within constraints on metabolite concentrations. Pathways with positive MDFs have bottleneck reactions that are thermodynamically feasible (i.e. with $\Delta_r G > 0$), so they are feasible overall. In contrast, pathways with negative MDFs have bottleneck reactions that are thermodynamically infeasible (i.e. with $\Delta_r G < 0$), so they are infeasible. See Materials and Methods for the MDF formulation, and discussion of concentration bounds used to find MDFs here.

We were able to find flux distributions with positive MDFs for all carbon sources for both growth and production modes without forced reassimilation - i.e. with unconstrained CO_2 exchange. However, we found differential sensitivity of MDFs to the constraint on RuBisCO flux for C2+ substrates. For most carbon sources, blocking RuBisCO flux either has no effect or is necessary for thermodynamically feasible biomass production (Fig S2). In particular, thermodynamically feasible biomass production from EG and 14BDO requires that RuBisCO flux be blocked, suggesting that reassimilation without additional reducing equivalents is not thermodynamically feasible for these substrates in the growth mode. Thus, there is no yield benefit to CO_2 reassimilation for these substrates (Fig. S1B), and reassimilation is thermodynamically infeasible anyway (Fig. S2).

PHB production is thermodynamically infeasible unless RuBisCO flux is blocked for fructose, succinate, and 14BDO, suggesting that reassimilation to produce PHB is infeasible in cells grown on these substrates unless additional reducing equivalents are available (Fig S2). This is again consistent with the observation that *C. necator* does not reassimilate CO_2 to an appreciable degree when it is grown on fructose or succinate alone; reassimilation to produce PHB is simply infeasible in these cases. Conversely, PHB production from EG and ethanol is only thermodynamically feasible when RuBisCO flux is allowed, suggesting that some reassimilation is required for stoichiometrically consistent, thermodynamically feasible PHB production from these substrates.

Growth and production mode MDFs with appropriate constraint on RuBisCO flux and without H_2-supported complete reassimilation are presented for all carbon sources in Fig. 2A. Growth MDFs for EG, 14BDO, and methanol are comparable to or higher than those of the native substrates CO_2 and formate, and significantly higher than those of the other carbon sources. This suggests that these substrates may be more efficient for biomass production than

CO_2/H_2 or formate. Production mode MDFs for all carbon sources are higher than growth mode MDFs, except in the cases of CO_2, acetate, and 14BDO.

Forcing complete reassimilation with H_2 oxidation results in significant changes to the production mode MDFs for all carbon sources (Fig. 2B). The MDFs for the forced reassimilation case are significantly lower than those of the unforced scenario for all carbon sources except acetate and ethanol. Indeed, for formate, succinate, adipate, EG, and methanol, the forced reassimilation scenario is only marginally thermodynamically feasible, since the MDFs for these carbon sources are near-zero. Thus, reassimilation of CO_2 generated by substrate oxidation is generally less favourable than CO_2 excretion. This strongly suggests that CO_2 reassimilation using electrons from H_2 is unlikely to be practically feasible. *C. necator* cells capable of reassimilation will be equally capable of excreting all CO_2 produced, yet excretion is more thermodynamically favourable for most carbon sources, even when sufficient H_2 for reassimilation is available. Therefore, for most carbon sources, CO_2-free fermentation via carbon reassimilation is unlikely to be practically achievable, even if it may be thermodynamically feasible.

For acetate and ethanol, however, the forced reassimilation scenario is as favourable or moreso than the scenario without forced assimilation. The two-step conversion of ethanol to acetyl-CoA does not produce CO_2, but it does produce excess reducing equivalents in the form of NADH (Fig. 2C). As such, de novo CO_2 assimilation is required to balance redox in the conversion of ethanol to PHB. Even without electrons from H_2, the conversion of ethanol to PHB is expected to be thermodynamically feasible and CO_2-negative, yielding 0.58 moles of PHB per mole of ethanol assimilated, or 116% of the maximum yield from ethanol alone. However, though ethanol is thermodynamically favourable as a CO_2-negative substrate, its practical application as such is likely limited because it is toxic to microbial cells. Previous work has shown that exposure of *C. necator* to sub-lethal concentrations of ethanol can improve PHB production by inducing redox stress that PHB production helps to balance [37]. As such, supplementation of ethanol may be a viable fermentation strategy, but it is likely not realistic as a primary feedstock for *C. necator*-based processes.

In the case of acetate, direct conversion to PHB with a complementary source of electrons does not actually require any CO_2 reassimilation. Acetate is converted to acetyl-CoA without carbon loss using energy from H_2 oxidation alone (Fig. 2D, lower panel). As such, this scenario is highly thermodynamically favourable and carbon efficient, yielding 0.5 moles of PHB per mole of acetate. Conversely, in the 'No Reassimilation' case for acetate, energy for PHB production is generated via the CO_2-producing TCA cycle (Fig. 2D, upper panel). This requires citrate lyase activity in the reverse direction, which is a known thermodynamic bottleneck in *C. necator* [33]. Indeed, we find that citrate lyase is expected to operate at the MDF of 2.58 $kJ \cdot mol^{-1}$ in this scenario. The citrate lyase bottleneck is avoided when electrons are available from H_2 instead. Hence, mixotrophic acetate-H_2 conversion to PHB is likely to be a feasible approach to CO_2-free fermentation. Unlike ethanol, acetate is a viable fermentation feedstock, so acetate-H_2 mixotrophic fermentation should be considered as a potential CO_2-free path to bioplastic production since it is strongly thermodynamically favourable and has a relatively low H_2 requirement.

Carbon-carbon mixotrophy can improve carbon yield and thermodynamic feasibility

Since CO_2-free carbon-H_2 mixotrophy is generally infeasible for the carbon sources examined here, we next aimed to evaluate the benefit and feasibility of carbon-carbon mixotrophies instead. Our rationale for doing so lies in the fact that the CO_2 generated from the fermentation of eCO_2R-derived carbon sources may ultimately be neutral in the global carbon balance. Therefore, mixotrophic scenarios making use of the electrons from these carbon sources could at least be net CO_2-neutral, even if these scenarios require CO_2 production at the point of fermentation. We built 90 models capable of using each possible pair of carbon sources by performing a pairwise addition of assimilation modules to each of the sole carbon source models we had generated previously. Then, we evaluated the carbon yield and MDF for PHB production using both carbon sources simultaneously to evaluate the viability of all possible synthetic mixotrophies. Yields and driving forces for all mixotrophic scenarios are presented in Fig. 3A, with the sole carbon source scenario along the diagonals.

For a given mixotrophic scenario to be viable, it must have a higher MDF than either sole consumption scenario, otherwise, sole consumption of the more thermodynamically favourable carbon source is more likely than mixotrophic consumption. In this situation, cells exposed to both carbon sources are more likely to primarily use one over the other, rather than both at the same time, even if they have been engineered to use both. Less critically, the mixotrophic carbon yield should be higher than that of either sole consumption case. For example, the carbon yield of EG-formate mixotrophy is 0.56 $mol \cdot mol^{-1}$, which is higher than that of formate alone (0.22 $mol \cdot mol^{-1}$), but not

EG alone (0.73 mol·mol^{-1}). Thus, transformation of EG alone is more carbon efficient than the mixotrophic scenario, so synthetic EG-formate mixotrophy may not be worth pursuing, depending on the source of either or both of the mixotrophic substrates.

Based on the MDF criterion, three carbon sources emerge as being broadly viable mixotrophy partners, as is highlighted in Fig. 3A. Formate, EG, and methanol all have MDFs in multiple pairings that are the same as the corresponding sole consumption cases, suggesting that mixotrophy is as thermodynamically favourable as the corresponding sole consumption scenarios. Formate is thermodynamically viable as a mixotrophic partner with fructose and EG, methanol is viable with glycerol and acetate, and EG is viable with fructose, acetate, and formate. Additionally, EG-methanol mixotrophy may be marginally viable, since the MDF of this pair (10.2 kJ·mol^{-1}) is within the range of uncertainty to that of EG alone (10.6 kJ·mol^{-1}).

When the carbon yields of these mixotrophies are considered, EG-acetate, and methanol-acetate emerge as the best mixotrophic strategies. Both mixotrophies yield a synergistic effect in that co-consumption improves efficiency relative to either corresponding sole consumption scenario. This synergy arises from the fact that mixotrophy with either EG or methanol enables all assimilated acetate to enter the PHB pathway without carbon loss for energy generation, similarly to acetate-H_2 mixotrophy (Fig. 2D). On top of that, both EG and methanol oxidation yield sufficient excess reducing equivalents to drive some carbon reassimilation - 0.3 mol·mol^{-1} for EG; 0.6 mol·mol^{-1} for methanol (Fig. S3). As a result of both of these effects, co-consumption with these substrates yields better carbon conservation than in the corresponding sole consumption scenarios.

If the co-substrates which are good mixotrophic pairs and can be derived from eCO_2R (formate, methanol, EG) are considered CO_2-neutral, then the carbon efficiency of PHB production for mixotrophic scenarios changes considerably, as shown in Fig 4. In this case, carbon yields greater than 1 mol·mol^{-1} are possible, because the carbon from the eCO_2R-derived co-substrate is "free"; it is essentially a carbon-based electron source replacing H_2. Though this is an idealization, it represents the best possible carbon efficiency for the metabolic system under consideration. Even in this idealized case, formate cannot support 100% carbon yield in any mixotrophic scenario, even though the viable ones (formate-fructose, formate-EG) have improved carbon yield relative to either sole consumption case. This is because formate can only produce a single reducing equivalent for every CO_2 molecule its oxidation yields, so there is a low cap on the carbon yield improvement that is possible with formate as a CO_2-neutral electron source.

In contrast, the thermodynamically viable methanol mixotrophic scenarios (methanol-acetate, methanol-glycerol, methanol-EG) all have carbon yields exceeding 1 mol·mol^{-1} if the carbon in methanol is not included in the yield. The methanol oxidation produces two reducing equivalents per CO_2 generated, and evidently this is sufficient to significantly improve the carbon yields of co-substrates. EG supports the most significant carbon yield improvements of all eCO_2R-derived electron sources, though, because its oxidation yields the most reducing equivalents. As a result, all thermodynamically viable EG mixotrophies have yields significantly greater than 1mol·mol^{-1} if the EG is considered to be CO_2-free. Indeed, the EG-methanol mixotrophy in which EG is the eCO_2R-derived carbon source has the highest carbon yield of all mixotrophic scenarios considered at 2.1 mol·mol^{-1}. Altogether, assimilation of a molecule each of EG and methanol yields eight reducing equivalents, which is sufficient to support the reassimilation of 1.66 molecules of CO_2 via the CBB. This represents a significant net negative CO_2 transformation if the reducing equivalents derived from EG are CO_2-neutral.

At present, eCO_2R cells tend to produce mixtures of at least a few of the carbon-based electron sources we consider. Thus, it is possible that the carbon yield for a number of these mixotrophic scenarios could be much higher than the values determined here, because the carbon intensity of *both* co-substrates could be very low. However, this would require the product mixture from the eCO_2R to contain carbon sources yielding feasible mixotrophies, which may be challenging given that ethanol mixotrophy is infeasible. In the case in which all carbon is low-CO_2 or CO_2-free, a more relevant constraint would be the rate at which conversion is possible in the mixotrophic scenarios. This would require estimating constraints on uptake rates for each mixotrophy, which is beyond the scope of the present work. However, our results do suggest that in hypothetical integrated electrochemical-fermentation processes, it might be worthwhile to "over-reduce" CO_2 to target EG and/or methanol production, if possible, because co-consumption of these substrates can enable significant improvements in downstream carbon efficiency relative to other, less reduced co-substrates.

Mixotrophy with partial oxidation is a viable strategy for low-CO_2 fermentation

Another strategy to increase carbon yield in carbon-carbon mixotrophies is to partially oxidize the electron-carrying co-substrate into a valuable exported intermediate. This is only possible with C2+ co-substrates with a partially oxidized intermediate that has value as a chemical product. Of the carbon sources investigated here, EG and glycerol meet these criteria. EG can be efficiently oxidized to glycolic acid (GA), yielding two reducing equivalents [38]. Glycolate dehydrogenase activity is required for GA to enter central carbon metabolism, so if this activity is blocked, excess GA is exported and accumulates externally instead of being assimilated (Fig. 5B). GA is a valuable commodity chemical that is used to produce a variety of products, such as cosmetics, coatings, adhesives, etc. Therefore, the development of low-CO_2 GA production routes is desirable [39].

A similar motif exists for glycerol, which can be oxidized in a two-step pathway to 3-hydroxypropionate (3HP). 3HP is also a valuable commodity for which sustainable production routes are actively sought [39]. Unlike GA, 3HP is not known to be assimilated into central carbon metabolism, but glycerol assimilation via glycerol kinase must be blocked for efficient conversion to 3HP instead (Fig. 5E). The first step in the glycerol-to-3HP pathway is commonly catalyzed by glycerol dehydratase, which requires cobalamin as a cofactor [40]. Though *C. necator* does not natively produce cobalamin [41], exogenous addition of this vitamin has been used to support heterologous glycerol dehydratase activity [42]. Therefore, we have included the pathway here to show the potential of its application in carbon conserving mixotrophy.

We added two new models in which EG and glycerol are partially oxidized and their respective acid products are exported to our existing suite of mixed models. In these models, EG and glycerol serve solely as electron sources; carbon for growth and production comes from CO_2 via the CBB cycle. We screened all models for their ability to feasibly support growth and production with H_2 uptake and CO_2 export blocked, but CO_2 import allowed. As expected, only the ethanol, GA, and 3HP models can support CO_2-consuming growth and production without electrons from H_2. In the GA model, $\sim$0.4 moles of CO_2 must be assimilated per mole of EG oxidized for both growth and production (Figs. 5B, S4), while for the 3HP model, $\sim$0.2 moles must be assimilated per mole of glycerol oxidized (Figs. 5E, S4). For all three sole substrates, growth and production modes are both thermodynamically viable, having positive MDFs (Fig. 5A). Remarkably, the MDF for production in both partial oxidation models is significantly higher than that of the CO_2/H_2 baseline, even though these models uses the same route for CO_2 assimilation. Coupling CO_2 utilization to EG or glycerol as an electron source significantly increases the minimum thermodynamic driving force compared to coupling to H_2 as an electron source.

The EG-to-GA and glycerol-to-3HP pathways could provide the necessary reducing equivalents to drive carbon conservative transformation of waste-derived carbon sources in mixotrophic scenarios. In such scenarios, partial oxidation of EG or glycerol would provide the electrons required for co-substrate conversion to PHB, and reassimilation of any CO_2 generated from co-substrate oxidation. We therefore examined each mixotrophic pairing with these pathways, with CO_2 efflux and H_2 input blocked. For both carbon sources, flux distributions with positive MDFs for both growth and production modes could be found for all mixotrophic scenarios (Fig. 5C, F), indicating that such mixotrophies are thermodynamically feasible.

Some mixotrophic scenarios with the GA model required additional CO_2 assimilation beyond reassimilation of carbon generated by oxidation of the co-substrate (Fig. S4). EG-acetate, EG-14BDO, EG-ethanol, and EG-methanol mixotrophies require de novo CO_2 assimilation when electrons are provided by the EG-to-GA pathway. This is unsurprising for the acetate mixotrophy, since we have already shown that complete EG oxidation provides sufficient reducing equivalents for acetate conversion to PHB. In the GA model, no CO_2 is generated from EG oxidation, so excess reducing equivalents are not required for carbon reassimilation, and instead drive de novo CO_2 assimilation. The glycerol-to-3HP pathway only supports additional CO_2 assimilation in the case of ethanol mixotrophy (Fig. S4). Ethanol utilization alone requires CO_2 assimilation (Fig. 2C), but coupling with both of the acid producing pathways increases the molar ratio of CO_2 uptake relative to the ethanol-only scenario because they provide additional reducing equivalents beyond the excess that ethanol oxidation produces.

To determine the practical viability of GA and 3HP mixotrophies, we compared their MDFs to those of the single carbon source scenario without forced reassimilation, and to those of the H_2-powered complete reassimilation scenario (Figs. 5D, G). MDFs are higher for GA model mixotrophies than for CO_2 excretion scenarios for acetate, fructose, and glycerol, suggesting that pairing the EG-to-GA pathway with these carbon sources is a feasible strategy to achieve full carbon reassimilation or better. Moreover, the MDFs for the EG-fructose and EG-glycerol mixotrophies are higher than those of the H_2-powered reassimilation case for the same carbon sources. This is not the case for

EG-acetate mixotrophy, for which H_2-powered reassimilation has a higher MDF (Fig. 5D). Similarly, MDFs for 3HP mixotrophies are higher than those for CO_2 excretion for acetate, fructose, EG, ethanol, and methanol. In all of these cases, the MDFs are also higher than for the comparable H_2-powered reassimilation scenario, though the acetate mixotrophy MDF is only marginally so (Fig. 5G).

These results suggest that mixotrophic fermentation with partial oxidation of either EG or glycerol could be a viable approach to CO_2-free upcycling of many of the waste streams examined here. Co-production of an acid renders carbon conservation viable because it provides CO_2-free electrons at the point of fermentation. Though there is a CO_2 cost to these electrons over the entire life cycle of the resulting outputs, reduction in carbon intensity at one step in that life cycle may be useful to reduce the overall carbon intensity. EG and glycerol are also more practical electron sources than H_2, because they are safer, and more miscible in water. Moreover, the practical feasibility of the acid-polymer co-production scenario is supported by the fact that the acids are exported while the polymer accumulates intracellularly. Biomass separation is a necessary downstream step of all bioprocesses, so recovery of both products is possible within the status quo approaches to downstream processing.

Discussion

We have shown that there there is significant potential to use *C. necator* as a catalyst to harvest electrons from waste-derived feedstocks to drive CO_2 utilization. This may provide a novel pathway to reducing the predicted high hydrogen requirement of a future circular carbon economy, while motivating the utilization of recalcitrant waste streams as inputs to chemical production. Critical to this potential is the native ability of *C. necator* to use CO_2 in response to excess available reducing equivalents from the oxidation of substrates with high DOR. This allows it to address redox imbalances by reducing CO_2 as required to store excess electrons in PHB. To date, this ability has primarily been exploited either by feeding *C. necator* CO_2/H_2 directly or formate as a sole eCO_2R-derived carbon source. We have uncovered several configurations which could enable significant improvements in carbon yield and thermodynamic feasibility compared to these status quo approaches to CO_2 utilization in *C. necator*.

Our analysis shows that acetate is critical to achieving thermodynamically feasible, high carbon yield mixotrophic fermentation. This is partly because of our choice of product, since acetyl-CoA is the input to the PHB pathway. However, a number of other valuable chemical products, such as short-chain fatty acids, can be derived from acetyl-CoA with energy input via reducing equivalents. Additionally, the partial oxidation scenarios we examined could yield low-CO_2 biopolymers beyond PHB without acid co-production because they generate intermediates which can be co-polymerized with 3-hydroxybutyrate. Both glycolate [43, 44] and 3-hydroxypropionate [45] co-polymers of 3-hydroxybutyrate have been demonstrated. Thus, while the present work is limited to a single polymer product, our focus on inputs may enable future work which considers production of a wide variety chemical products using low-CO_2 mixotrophies.

We did not consider any metabolic rewiring to improve efficiency in our analysis, because doing so would have expanded the design space to an impractical degree. Yet, improvements to thermodynamic driving forces via rewiring have been shown in *C. necator* [33], and carbon yield improvements for sugar assimilation via the NOG pathway have been demonstrated in other host organisms [46]. These - and other, as-yet undescribed strategies - could be applied in the mixotrophic scenarios we have evaluated here to further improve carbon conservation and thermodynamic feasibility. The present work may help to limit the design scope for metabolic rewiring approaches, since we have shown non-viability of a number of synthetic mixotrophies. Future work should focus on the viable combinations we have elucidated, namely those making use of acetate for carbon and EG or methanol for reducing equivalents.

Practically, achieving mixotrophy in a *C. necator* platform - or any microbe, for that matter - will be challenging. In the wild, access to single carbon sources is often limited; a ready supply of two or more at the same time would be exceedingly rare. As such, complex metabolic regulatory systems have evolved to prioritize the use of limited cellular resources for sequential carbon source utilization over co-consumption. These regulatory systems present a significant barrier to achieving the proposed synthetic mixotrophies. Despite these challenges, synthetic, CO_2-utilizing mixotrophy has been demonstrated in *Escherichia coli* previously [47, 48]. *C. necator* may be a better platform for the establishment of synthetic mixotrophy than other industrial microbes because it seemingly maintains continual expression of proteins required for assimilation of many different carbon sources in preparation for environmental shifts [34]. However, it is still known to use global regulators to prioritize high-quality carbon sources over low-quality ones [49]. Moreover, regulation of PHB production is known to influenced by nutrient availability, which may have

unintended interactions with the proposed assimilation pathway. Thus, experimental work to understand how global regulators could be manipulated and/or circumvented will likely be required to build strains capable of the mixotrophies proposed here.

Materials and Methods

Curation of complementary feedstocks

A literature search was performed to establish a list of compounds which could reasonably be used mixotrophically. Complementary feedstocks which could be derived from eCO_2R and/or those which are monomers of plastics and/or those which are byproducts of other bioprocesses were considered. For example, glycerol is a byproduct of biodiesel production [50], so it was included. Only feedstocks with characterized assimilation pathways could be included. Anaerobic assimilation pathways were excluded. This yielded a list of six alternative feedstocks (ethylene glycol, methanol, adipate, 1,4-butanediol, and ethanol) and four that have already been reported for *C. necator* (CO_2, formate, fructose, succinate). All feedstocks are presented in Table 1, along with their sources, assimilation pathways, and references to literature in which these pathways are described.

Degree of reduction (DOR), defined here as the number of electrons per carbon atom which could be released via oxidation was calculated as follows for each carbon source:

$$\mathrm{DOR} = \frac{4n_C + n_H - 2n_O}{n_C} \tag{1}$$

where n_C, n_H, and n_O are, respectively, the number of carbon, hydrogen, and oxygen atoms in the molecule. The DOR for each carbon source was determined and is similarly presented in Table 1.

Model building and modification

The core model constructed by Janasch, *et al* [33] was modified to establish a starting point from which mixotrophy-capable models were generated. The original core model does not include hydrogenase activity, so soluble (SH) and membrane hydrogenase (MH) reactions were added. The SH converts H_2 and NAD+ into NADH and a proton, while the MH converts H_2 and ubiquinone to ubiquinol. Additionally, the fructose and formate transport reactions in the original model were removed for convenience based on the downstream workflow. Finally, the non-native phosphoketolase and ATP-citrate lyase reactions were kept in the model, but were blocked for all analyses. These reactions were added by Janasch, *et al* to address thermodynamic bottlenecks that they uncovered through their analysis. Since they are not present in wild-type *C. necator*, they were excluded. These modifications yielded a baseline model capable of growing only on CO_2 and H_2.

From here, uptake and assimilation pathways for all ten carbon sources were individually added to the baseline model using the COBRApy package in Python3 to produce ten unique models capable of assimilating a single carbon source other than CO_2. Multiple models were constructed, rather than a single model capable of using multiple carbon sources, to avoid spurious overlap between assimilation routes. Each model was evaluated for its ability to produce biomass solely using the complementary carbon source to ensure that the curated assimilation pathways were viable. The uptake of the carbon source for each model was constrained to a value of 1 mmol·gCDW^{-1}·h^{-1} and H_2 uptake was blocked, then parsimonious flux balance analysis (pFBA) was used with biomass as the objective function to find the maximum biomass yield, $Y_{X/S}^{max}$. Initially, butyrate was considered among the possible alternative substrates, but its assimilation pathway could not support growth as a sole carbon source, so it was excluded at this stage.

Carbon-H_2 mixotrophy

Production envelopes were generated by varying the lower bound on the flux through the biomass reaction between 0 and $Y_{X/S}^{max}$ for an uptake rate of 1 mmol·gCDW^{-1}·h^{-1} and finding the optimal PHB yield, $Y_{P/S}$, for each intermediate biomass yield. pFBA with the PHB export reaction as the objective function was used to find $Y_{P/S}$ along the production envelope. This was performed first with H_2 uptake blocked and CO_2 export unconstrained, then with H_2

uptake unconstrained, but CO_2 export blocked to force complete reassimilation of carbon. The H_2 requirements for operation at $Y_{X/S}^{max}$ and the maximum PHB yield, $Y_{P/S}^{max}$, were determined by finding the ratio of H_2 uptake to flux through RuBisCO at these points of the production envelopes. For acetate and ethanol, RuBisCO flux is not required for operation at $Y_{P/S}^{max}$, so the H_2/CO_2 value was set to 0 for these carbon sources in the production mode.

The expected H_2 cost in Fig. 1E was determined by:

$$\frac{q_{H_2}}{v_{\text{RUBISCO}}} = \frac{\text{DOR}_{\text{PHB}} - Y_{\text{NAD(P)H/DOR}} \cdot \text{DOR}_C}{v_{\text{RUBISCO}/n_C}} = \frac{4.5 - 0.5\text{DOR}_C}{1.5} \tag{2}$$

Where 4.5 corresponds to the DOR of PHB, DOR_{PHB}. For each degree of reduction of the carbon source, DOR_C, one fewer half-mole of H_2 is required to reassimilate CO_2, because the yield of reducing equivalents per DOR, $Y_{\text{NAD(P)H/DOR}}$, is 0.5 (i.e. each DOR can be converted to one half mole of reducing equivalent). The value of the denominator accounts for the fact that complete reassimilation requires 1.5 mol of flux through RuBisCO for every mole of CO_2 converted to PHB because pyruvate dehydrogenase produces 0.5 mole of CO_2 in addition to the CO_2 derived from the substrate.

Max-min driving force estimation

The maximum-minimum thermodynamic driving force (MDF) was determined using the OptMDFPathway package [51] in Python3 with the pH set to 7.4, pMg at 3, ionic strength at 200 mM, and at a temperature of 30°C. Briefly, finding the MDF for a given set of reactions involving metabolites with log-transformed concentrations, x_i, requires solving the linear optimization problem:

$$\begin{aligned} \underset{B,\vec{x}}{\text{maximize}} \quad & B \\ \text{subject to} \quad & -(\Delta_r \mathbf{G}'^{\circ} + RT \cdot \mathbf{S}^T \vec{x}) \geq B \\ & \ln c_{i,min} \leq x_i \leq \ln c_{i,max} \quad i = 1, \ldots, n \end{aligned}$$

Where B is the minimum driving force for all reactions in a pathway. The optimized value of B is the MDF, at which multiple reactions in a pathway may operate. $\Delta_r \mathbf{G}'^{\circ}$ is a vector containing the standard Gibbs energy of the pathway reactions, $\mathbf{S}$ is the stoichiometric matrix describing the active reactions of the pathway, $\vec{x}$ is the vector of log-transformed metabolite concentrations, and $c_{i,min}$ and $c_{i,max}$ are the upper and lower bounds on concentrations for metabolite i of n total metabolites involved in the pathway.

The lower and upper bounds on internal metabolite concentrations were set to $c_{i,min} = 1$ μM and $c_{i,max} = 10$ mM, and standard Gibbs free energies for reactions were determined using the component contribution method included in the OptMDFPathway package. Transport reactions were excluded from all MDF calculations for simplicity. Accurately capturing transport reactions in the MDF formulation hinges on having good estimates of the bounds on concentrations in specific compartments, which is challenging. Thus, these reactions were excluded to avoid unjustified assumptions. Similarly, the biomass and PHB reactions were excluded because, as terminal reactions that inherently do not operate at steady-state, it is not clear how they can be included in the MDF framework. Biomass and PHB accumulation, as well as transport of the carbon sources examined here, are all known to occur spontaneously, so it was assumed that they are thermodynamically feasible in the conditions examined.

Sensitivity to RuBisCO flux

The yield sensitivity of each sole consumption model to forced RuBisCO flux was determined by setting the uptake flux of the corresponding carbon source to 1 mmol·gCDW^{-1}·h^{-1} and varying the lower bound on flux through the RUBISCO reaction between 0 and n_C. H_2 transport was blocked and CO_2 transport was unconstrained. At each forced RUBISCO flux, pFBA was performed with either the biomass or PHB export reaction as the objective. This approach was used to generate Fig. S1A.

Flux distributions determined with pFBA may include an active RUBISCO reaction, because carbon reassimilation increases the value of the objective function. However, this may not be thermodynamically feasible. The thermodynamic sensitivity to RuBisCO flux was determined by setting the bounds on the RUBISCO reaction to

zero or allowing unconstrained flux in the forward direction. The optimal biomass or PHB production yield was found using pFBA with unconstrained CO_2 export and H_2 transport constrained to zero for both sets of bounds on RUBISCO flux. Then MDFs were calculated as described for both the growth-only and production-only extremes. This approach was used to generate Fig. S2.

Carbon-carbon mixotrophic performance

Mixotrophic models were constructed through pairwise addition of consumption modules to each sole carbon source model, without repeat, since the order in which the consumption modules are combined does not matter (e.g. EG-Acetate is the same as Acetate-EG). Uptake rates for each carbon source were constrained to a maximum of 1 $\text{mmol}\cdot\text{gCDW}^{-1}\cdot\text{h}^{-1}$, such that a total uptake rate of 2 $\text{mmol}\cdot\text{gCDW}^{-1}\cdot\text{h}^{-1}$ was possible in each mixotrophic case. All mixotrophic yields were normalized to total carbon uptake to account for this. The yields presented in Fig. 3 were determined according to:

$$Y_{\text{PHB/S}}\ [\text{C-mol/C-mol}] = \frac{4 \cdot v_{\text{PHB}}}{n_{C1} \cdot v_{C1} + n_{C2} \cdot v_{C2}} \tag{3}$$

where v_{PHB} is the flux through the PHB synthesis reaction, n_C is the carbon number of each substrate, and v_C is the uptake flux of each carbon source. When one of the carbon sources was considered CO_2-free, its contribution to the yield was simply omitted.

The same uptake bounds and pFBA optimization approach were used to find MDFs for the mixotrophic models. In the case of the EG-to-GA and glycerol-to-3HP models, the appropriate export and transport reactions of the either consumption model were unconstrained, whereas the reactions required for assimilation into central carbon metabolism were constrained to zero flux. pFBA was then used to find optimized flux distributions, as described.

Code and Data Availability

Consumption modules corresponding to those listed in Table 1 for each carbon source which can yield both biomass and PHB are included in the Supplementary Information, along with the curated core model. All data and code used for analysis and visualization are available at github.com/theL-A-B

Acknowledgments

We acknowledge that this work was carried out on the traditional territory of the Attawandaron, Anishinaabeg and Haudenosaunee peoples. The University of Waterloo is situated on the Haldimand Tract, the land promised to the Six Nations that includes ten kilometers on each side of the Grand River.

Conflict of Interest

The authors declare no competing interests

Funding

This work was funded in part by the NSERC Alliance Global Centers program through grant ALLRP 597254-24.

Consent to Publish

Consent to publish declaration: not applicable.

Consent to Participate

Consent to participate declaration: not applicable.

Ethics Declaration

Ethics declaration: not applicable.

References

1. "Climate change 2021: The physical science basis," tech. rep., Intergovernmental Panel on Climate Change, 2021.

2. S. V. Mohan, S. Dahiya, K. Amulya, R. Katakojwala, and T. K. Vanitha, "Can circular bioeconomy be fueled by waste biorefineries — a closer look," *Bioresource Technology Reports*, vol. 7, p. 100277, 9 2019.

3. E. Stephens, I. L. Ross, J. H. Mussgnug, L. D. Wagner, M. A. Borowitzka, C. Posten, O. Kruse, and B. Hankamer, "Future prospects of microalgal biofuel production systems," *Trends in Plant Science*, vol. 15, pp. 554–564, 10 2010.

4. U. Nyambuu and W. Semmler, "Limits on the extraction of fossil fuels," *Contributions to Economics*, vol. Part F32, pp. 59–69, 2023.

5. S. A. Farooqi, A. S. Farooqi, S. Sajjad, C. Yan, and A. B. Victor, "Electrochemical reduction of carbon dioxide into valuable chemicals: a review," *Environmental Chemistry Letters 2023 21:3*, vol. 21, pp. 1515–1553, 1 2023.

6. D. S. Mallapragada, Y. Dvorkin, M. A. Modestino, D. V. Esposito, W. A. Smith, B.-M. Hodge, M. P. Harold, V. M. Donnelly, A. Nuz, C. Bloomquist, K. Baker, L. C. Grabow, Y. Yan, N. N. Rajput, R. L. Hartman, E. J. Biddinger, E. S. Aydil, and A. D. Taylor, "Decarbonization of the chemical industry through electrification: Barriers and opportunities," *Joule*, vol. 7, pp. 23–41, 1 2023.

7. A. Kätelhön, R. Meys, S. Deutz, S. Suh, and A. Bardow, "Climate change mitigation potential of carbon capture and utilization in the chemical industry," *Proceedings of the National Academy of Sciences of the United States of America*, vol. 166, pp. 11187–11194, 6 2019.

8. D. Saygin and D. Gielen, "Zero-emission pathway for the global chemical and petrochemical sector," *Energies*, vol. 14, p. 3772, 7 2021.

9. F. Meng, A. Wagner, A. B. Kremer, D. Kanazawa, J. J. Leung, P. Goult, M. Guan, S. Herrmann, E. Speelman, P. Sauter, S. Lingeswaran, M. M. Stuchtey, K. Hansen, E. Masanet, A. C. Serrenho, N. Ishii, Y. Kikuchi, and J. M. Cullen, "Planet-compatible pathways for transitioning the chemical industry," *Proceedings of the National Academy of Sciences of the United States of America*, vol. 120, p. e2218294120, 2 2023.

10. R. A. Tufa, D. Chanda, M. Ma, D. Aili, T. B. Demissie, J. Vaes, Q. Li, S. Liu, and D. Pant, "Towards highly efficient electrochemical co2 reduction: Cell designs, membranes and electrocatalysts," *Applied Energy*, vol. 277, p. 115557, 11 2020.

11. K. U. Calvinho, A. B. Laursen, K. M. Yap, T. A. Goetjen, S. Hwang, N. Murali, B. Mejia-Sosa, A. Lubarski, K. M. Teeluck, E. S. Hall, E. Garfunkel, M. Greenblatt, and G. C. Dismukes, "Selective co2 reduction to c3 and c4 oxyhydrocarbons on nickel phosphides at overpotentials as low as 10 mv," *Energy Environmental Science*, vol. 11, pp. 2550–2559, 9 2018.

12. L. Rui, L. Ting, R. García-Muelas, A. J. Martín, L. P. Veenstra, S. Tze, J. Chen, Y. Peng, E. Yu, X. Per, S. Pablo-García, N. López, J. P.-R. U. Boon, and S. Yeo, "Electrochemical reduction of carbon dioxide to 1-butanol on oxide-derived copper," *Angewandte Chemie*, vol. 132, pp. 21258–21265, 11 2020.

13. C. Wang, Z. Lv, X. Feng, W. Yang, and B. Wang, "Recent advances in electrochemical co2-to-multicarbon conversion: From fundamentals to industrialization," *Advanced Energy Materials*, vol. 13, p. 2302382, 12 2023.

14. Y. Liu and X.-B. Lu, "Current challenges and perspectives in co2-based polymers," *Macromolecules*, pp. 1759–1777, 2023.

15. C. G. Okoye-Chine, K. Otun, N. Shiba, C. Rashama, S. N. Ugwu, H. Onyeaka, and C. T. Okeke, "Conversion of carbon dioxide into fuels—a review," *Journal of CO2 Utilization*, vol. 62, 8 2022.

16. F. E. Liew, R. Nogle, T. Abdalla, B. J. Rasor, C. Canter, R. O. Jensen, L. Wang, J. Strutz, P. Chirania, S. D. Tissera, A. P. Mueller, Z. Ruan, A. Gao, L. Tran, N. L. Engle, J. C. Bromley, J. Daniell, R. Conrado, T. J. Tschaplinski, R. J. Giannone, R. L. Hettich, A. S. Karim, S. D. Simpson, S. D. Brown, C. Leang, M. C. Jewett, and M. Köpke, "Carbon-negative production of acetone and isopropanol by gas fermentation at industrial pilot scale," *Nature Biotechnology 2022 40:3*, vol. 40, pp. 335–344, 2 2022.

17. L. G. Ljungdahl, "The autotrophic pathway of acetate synthesis in acetogenic bacteria," *Annual Review of Microbiology*, vol. 40, pp. 415–450, 10 1986.

18. S. W. Ragsdale, "Enzymology of the wood–ljungdahl pathway of acetogenesis," *Annals of the New York Academy of Sciences*, vol. 1125, pp. 129–136, 3 2008.

19. A. P. Carvalho, S. O. Silva, J. M. Baptista, and F. X. Malcata, "Light requirements in microalgal photobioreactors: An overview of biophotonic aspects," *Applied Microbiology and Biotechnology*, vol. 89, pp. 1275–1288, 3 2011.

20. A. D. Kroumov, M. M. Zaharieva, F. B. Scheufele, V. Balabanova, and H. Najdenski, "Engineering challenges of carbon dioxide capture and sequestration by cyanobacteria," *Ecophysiology and Biochemistry of Cyanobacteria*, pp. 351–372, 1 2022.

21. F. Reinecke and A. Steinbüchel, "Ralstonia eutropha strain h16 as model organism for pha metabolism and for biotechnological production of technically interesting biopolymers," *Journal of Molecular Microbiology and Biotechnology*, vol. 16, pp. 91–108, 12 2009.

22. J. Panich, B. Fong, and S. W. Singer, "Metabolic engineering of cupriavidus necator h16 for sustainable biofuels from co2," *Trends in Biotechnology*, vol. 39, pp. 412–424, 4 2021.

23. H. Salehizadeh, N. Yan, and R. Farnood, "Recent advances in microbial co2 fixation and conversion to value-added products," *Chemical Engineering Journal*, vol. 390, p. 124584, 6 2020.

24. R. Cramm, "Genomic view of energy metabolism in ralstonia eutropha h16," *Journal of molecular microbiology and biotechnology*, vol. 16, pp. 38–52, 10 2009.

25. P. Stegmann, V. Daioglou, M. Londo, D. P. van Vuuren, and M. Junginger, "Plastic futures and their co2 emissions," *Nature*, vol. 612, pp. 272–276, 12 2022.

26. R. Sirohi, J. S. Lee, B. S. Yu, H. Roh, and S. J. Sim, "Sustainable production of polyhydroxybutyrate from autotrophs using co2 as feedstock: Challenges and opportunities," *Bioresource Technology*, vol. 341, p. 125751, 12 2021.

27. C. A. Villa, J. Marienhagen, S. Noack, and S. A. Wahl, "Achieving net zero co2 emission in the biobased production of reduced platform chemicals using defined co-feeding of methanol," *Current Opinion in Biotechnology*, vol. 82, p. 102967, 8 2023.

28. S. W. Jones, A. G. Fast, E. D. Carlson, C. A. Wiedel, J. Au, M. R. Antoniewicz, E. T. Papoutsakis, and B. P. Tracy, "Co 2 fixation by anaerobic non-photosynthetic mixotrophy for improved carbon conversion," *Nature Communications*, vol. 7, 9 2016.

29. C. A. Vees, C. Herwig, and S. Pflügl, "Mixotrophic co-utilization of glucose and carbon monoxide boosts ethanol and butanol productivity of continuous clostridium carboxidivorans cultures," *Bioresource Technology*, vol. 353, p. 127138, 6 2022.

30. H. Schulz-Mirbach, J. L. Krüsemann, T. Andreadaki, J. N. Nerlich, E. Mavrothalassiti, S. Boecker, P. Schneider, M. Weresow, O. Abdelwahab, N. Paczia, B. Dronsella, T. J. Erb, A. Bar-Even, S. Klamt, and S. N. Lindner, "Engineering new-to-nature biochemical conversions by combining fermentative metabolism with respiratory modules," *Nature Communications*, vol. 15, 12 2024.

31. W. A. van Winden, R. Mans, S. Breestraat, R. A. Verlinden, Álvaro Mielgo-Gómez, E. A. de Hulster, H. M. de Bruijn, and H. J. Noorman, "Towards closed carbon loop fermentations: Cofeeding of yarrowia lipolytica with glucose and formic acid," *Biotechnology and Bioengineering*, vol. 119, pp. 2142–2151, 8 2022.

32. J. B. A. Arends, S. A. Patil, H. Roume, and K. Rabaey, "Continuous long-term electricity-driven bioproduction of carboxylates and isopropanol from co2 with a mixed microbial community," *Journal of CO2 Utilization*, vol. 20, pp. 141–149, 2017.

33. M. Janasch, N. Crang, J. Asplund-Samuelsson, E. Sporre, M. Bruch, A. Gynnå, M. Jahn, and E. P. Hudson, "Thermodynamic limitations of phb production from formate and fructose in cupriavidus necator," *Metabolic Engineering*, vol. 73, pp. 256–269, 9 2022.

34. M. Jahn, N. Crang, M. Janasch, A. Hober, B. Forsström, K. Kimler, A. Mattausch, Q. Chen, J. Asplund-Samuelsson, and E. P. Hudson, "Protein allocation and utilization in the versatile chemolithoautotroph cupriavidus necator," *eLife*, p. e69019, 2021.

35. Y. Zhang, J. Jiang, Y. Zhang, W. Wang, X. Cao, and C. Li, "The carbon source effect on the production of ralstonia eutropha h16 and proteomic response underlying targeting the bioconversion with solar fuels," *Applied Biochemistry and Biotechnology*, vol. 194, pp. 3212–3227, 7 2022.

36. S. Al-Ani and Y. Kim, "Carbon preference by cupriavidus necator for growth and accumulation phases: Heterotrophic vs. autotrophic metabolisms," *Journal of Power Sources*, vol. 626, p. 235797, 1 2025.

37. S. Obruca, I. Marova, Z. Svoboda, and R. Mikulikova, "Use of controlled exogenous stress for improvement of poly(3-hydroxybutyrate) production in cupriavidus necator," *Folia Microbiologica*, vol. 55, pp. 17–22, 2010.

38. A. V. Pandit, E. Harrison, and R. Mahadevan, "Engineering escherichia coli for the utilization of ethylene glycol," *Microbial Cell Factories*, vol. 20, pp. 1–17, 12 2021.

39. J. Becker, A. Lange, J. Fabarius, and C. Wittmann, "Top value platform chemicals: bio-based production of organic acids," *Current Opinion in Biotechnology*, vol. 36, pp. 168–175, 12 2015.

40. A. Kalantari, T. Chen, B. Ji, I. A. Stancik, V. Ravikumar, D. Franjevic, C. Saulou-Bérion, A. Goelzer, and I. Mijakovic, "Conversion of glycerol to 3-hydroxypropanoic acid by genetically engineered bacillus subtilis," *Frontiers in Microbiology*, vol. 8, p. 254491, 4 2017.

41. A. Salinas, C. McGregor, V. Irorere, C. Arenas-López, R. R. Bommareddy, K. Winzer, N. P. Minton, and K. Kovács, "Metabolic engineering of cupriavidus necator h16 for heterotrophic and autotrophic production of 3-hydroxypropionic acid," *Metabolic Engineering*, vol. 74, pp. 178–190, 11 2022.

42. C. McGregor, N. P. Minton, and K. Kovács, "Biosynthesis of poly(3hb- co-3hp) with variable monomer composition in recombinant cupriavidus necator h16," *ACS synthetic biology*, vol. 10, pp. 3343–3352, 12 2021.

43. H. Tomita, K. Satoh, C. T. Nomura, and K. Matsumoto, "Biosynthesis of poly(glycolate-co-3-hydroxybutyrate-co-3-hydroxyhexanoate) in escherichia coli expressing sequence-regulating polyhydroxyalkanoate synthase and medium-chain-length 3-hydroxyalkanoic acid coenzyme a ligase," *Bioscience, biotechnology, and biochemistry*, vol. 86, pp. 217–223, 2 2022.

44. Z. J. Li, K. Qiao, W. Shi, B. Pereira, H. Zhang, B. D. Olsen, and G. Stephanopoulos, "Biosynthesis of poly(glycolate-co-lactate-co-3-hydroxybutyrate) from glucose by metabolically engineered escherichia coli," *Metabolic Engineering*, vol. 35, pp. 1–8, 5 2016.

45. M. Li, W. Li, T. Zhang, K. Guo, D. Feng, F. Liang, C. Xu, M. Xian, and H. Zou, "De novo synthesis of poly(3-hydroxybutyrate-co-3-hydroxypropionate) from oil by engineered cupriavidus necator," *Bioengineering 2023, Vol. 10, Page 446*, vol. 10, p. 446, 4 2023.

46. I. W. Bogorad, T. S. Lin, and J. C. Liao, "Synthetic non-oxidative glycolysis enables complete carbon conservation," *Nature*, vol. 502, pp. 693–697, 2013.

47. N. Antonovsky, S. Gleizer, E. Noor, Y. Zohar, E. Herz, U. Barenholz, L. Zelcbuch, S. Amram, A. Wides, N. Tepper, D. Davidi, Y. Bar-On, T. Bareia, D. Wernick, I. Shani, S. Malitsky, G. Jona, A. Bar-Even, and R. Milo, "Sugar synthesis from co2 in escherichia coli," *Cell*, vol. 166, pp. 115–125, 6 2016.

48. S. Gleizer, R. Ben-Nissan, Y. M. Bar-On, N. Antonovsky, E. Noor, Y. Zohar, G. Jona, E. Krieger, M. Shamshoum, A. Bar-Even, and R. Milo, "Conversion of escherichia coli to generate all biomass carbon from co2," *Cell*, vol. 179, pp. 1255–1263.e12, 11 2019.

49. C. H. Calvey, V. S. i Nogué, A. M. White, C. M. Kneucker, S. P. Woodworth, H. M. Alt, C. A. Eckert, and C. W. Johnson, "Improving growth of cupriavidus necator h16 on formate using adaptive laboratory evolution-informed engineering," *Metabolic Engineering*, vol. 75, pp. 78–90, 2023.

50. C. R. Chilakamarry, A. M. M. Sakinah, A. W. Zularisam, A. Pandey, and D.-V. N. Vo, "Technological perspectives for utilisation of waste glycerol for the production of biofuels: A review," *Environmental Technology Innovation*, vol. 24, p. 101902, 2021.

51. O. Hädicke, A. von Kamp, T. Aydogan, and S. Klamt, "Optmdfpathway: Identification of metabolic pathways with maximal thermodynamic driving force and its application for analyzing the endogenous co2 fixation potential of escherichia coli," *PLOS Computational Biology*, vol. 14, p. e1006492, 9 2018.

52. M. Zhao, G. Li, and Y. Deng, "Engineering escherichia coli for glutarate production as the c5 platform backbone," *Applied and Environmental Microbiology*, vol. 84, pp. e00814–18, 8 2018.

53. A. Pohlmann, W. F. Fricke, F. Reinecke, B. Kusian, H. Liesegang, R. Cramm, T. Eitinger, C. Ewering, M. Pötter, E. Schwartz, A. Strittmatter, I. Voß, G. Gottschalk, A. Steinbüchel, B. Friedrich, and B. Bowien, "Genome sequence of the bioplastic-producing "knallgas" bacterium ralstonia eutropha h16," *Nature Biotechnology 2006 24:10*, vol. 24, pp. 1257–1262, 9 2006.

54. N. Pearcy, M. Garavaglia, T. Millat, J. P. Gilbert, Y. Song, H. Hartman, C. Woods, C. Tomi-Andrino, R. R. Bommareddy, B. K. Cho, D. A. Fell, M. Poolman, J. R. King, K. Winzer, J. Twycross, and N. P. Minton, "A genome-scale metabolic model of cupriavidus necator h16 integrated with tradis and transcriptomic data reveals metabolic insights for biotechnological applications," *PLOS Computational Biology*, vol. 18, p. e1010106, 5 2022.

55. W. J. Li, T. Narancic, S. T. Kenny, P. J. Niehoff, K. O'Connor, L. M. Blank, and N. Wierckx, "Unraveling 1,4-butanediol metabolism in pseudomonas putida kt2440," *Frontiers in Microbiology*, vol. 11, p. 382, 3 2020.

56. H. Liang, X. Ma, W. Ning, Y. Liu, A. J. Sinskey, G. Stephanopoulos, and K. Zhou, "Constructing an ethanol utilization pathway in escherichia coli to produce acetyl-coa derived compounds," *Metabolic Engineering*, vol. 65, pp. 223–231, 5 2021.

57. P. A. Sanford and B. M. Woolston, "Synthetic or natural? metabolic engineering for assimilation and valorization of methanol," *Current Opinion in Biotechnology*, vol. 74, pp. 171–179, 4 2022.

58. H. Löwe and A. Kremling, "In-depth computational analysis of natural and artificial carbon fixation pathways," *BioDesign Research*, vol. 2021, 2021.

Table 1. Consumption modules used to construct *C. necator* models capable of consuming alternative substrates. See supplemental material for reaction codes. PBS: polybutylene succinate; PBAT: polybutylene adipate succinate; PET: polyethylene terephthalate

Carbon Source	DOR	Assimilation Reactions	Ref.	Source(s)
Formate	2	FDH: formate + NAD+ + H_2O = CO_2 + NADH	[33]	eCO_2R
Succinate	3.5	SUCD[1]: succinate + ubiquinone = fumarate + ubiquinol	[33]	Sugar fermentation PBS depol.
Acetate	4	ACS[1]: acetate + CoA + ATP = acetyl-CoA + PPi + AMP ACK[1]: acetate + ATP = ADP + acetyl-phosphate	[33]	Acetogenic fermentation
Adipate	4.33	ACL: adipate + ATP + CoA = adipyl-CoA + ADP + Pi ACDH: adipyl-CoA + ubiquinone = 5-carboxy-2-pentenoyl-CoA + ubiquinol CEDH: 5-carboxy-2-pentenoyl-CoA + H_2O = 3-hydroxyadipyl-CoA HADH: 3-hydroxyadipyl-CoA + NAD+ = 3-ketoadipyl-CoA + NADH OAT: 3-ketoadipyl-CoA + CoA = acetyl-CoA + succinyl-CoA	[52] [53]	Sugar fermentation PBAT depol.
Glycerol	4.67	GLYK: glycerol + ATP = glycerol-3-phosphate + ADP GKDH: glycerol-3-phosphate + ubiquinone = dihydroxyacetone phosphate + ubiquinol GLDH[2]: glycerol = 3-hydroxypropanal + H_2O HPADH[2]: 3-hydroxypropanal + NADP+ + H_2O = 3-hydroxypropionate + NADPH	[40] [54]	Biodiesel side stream
Ethylene glycol	5	GAR: ethylene glycol + NAD+ = glycoaldehyde + NADH GAD: glycoaldehyde + NAD+ + H_2O = glycolic acid + NADH GDH: glycolic acid + ubiquinone = glyoxylate + ubiquinol GCL: 2 glyoxylate + H_2O = tartronate semialdehyde + CO_2 TSR: tartronate semialdehyde + NADH = NAD+ + glycerate G2K: glycerate + ATP = 2-phosphoglycerate + ADP	[38]	Sugar fermentation side stream eCO_2R PET depol.
1,4-Butanediol	5.5	ADH: 1,4-butanediol + NAD+ = 4-hydroxybutyraldehyde + NADH BDH: 4-hydroxybutyraldehyde + CoA + NAD+ = 4-hydroxybutyryl-CoA + NADH COAT: 4-hydroxybutyryl-CoA + acetate = acetyl-CoA + 4-hydroxybutyrate HBD: 4-hydroxybutyrate + NAD = succinate semialdehyde + NADH SSADH: succinate semialdehyde + NAD + CoA = NADH + succinyl-CoA	[55]	PBAT depol.
Ethanol	6	EDG: ethanol + NAD+ = acetaldehyde + NADH ACEDH: acetaldehyde + NAD+ + CoA = acetyl-CoA + NADH	[56]	eCO_2R
Methanol	6	METDH: methanol + NAD+ = formaldehyde + NADH FADH: formaldehyde + NAD+ + H_2O = formate + NADH FDH: formate + NAD+ + H_2O = CO_2 + NADH	[57] [58]	eCO_2R

[1] - reaction is already present in the core *C. necator* model
[2] - required for the glycerol-to-3HP scenarios only

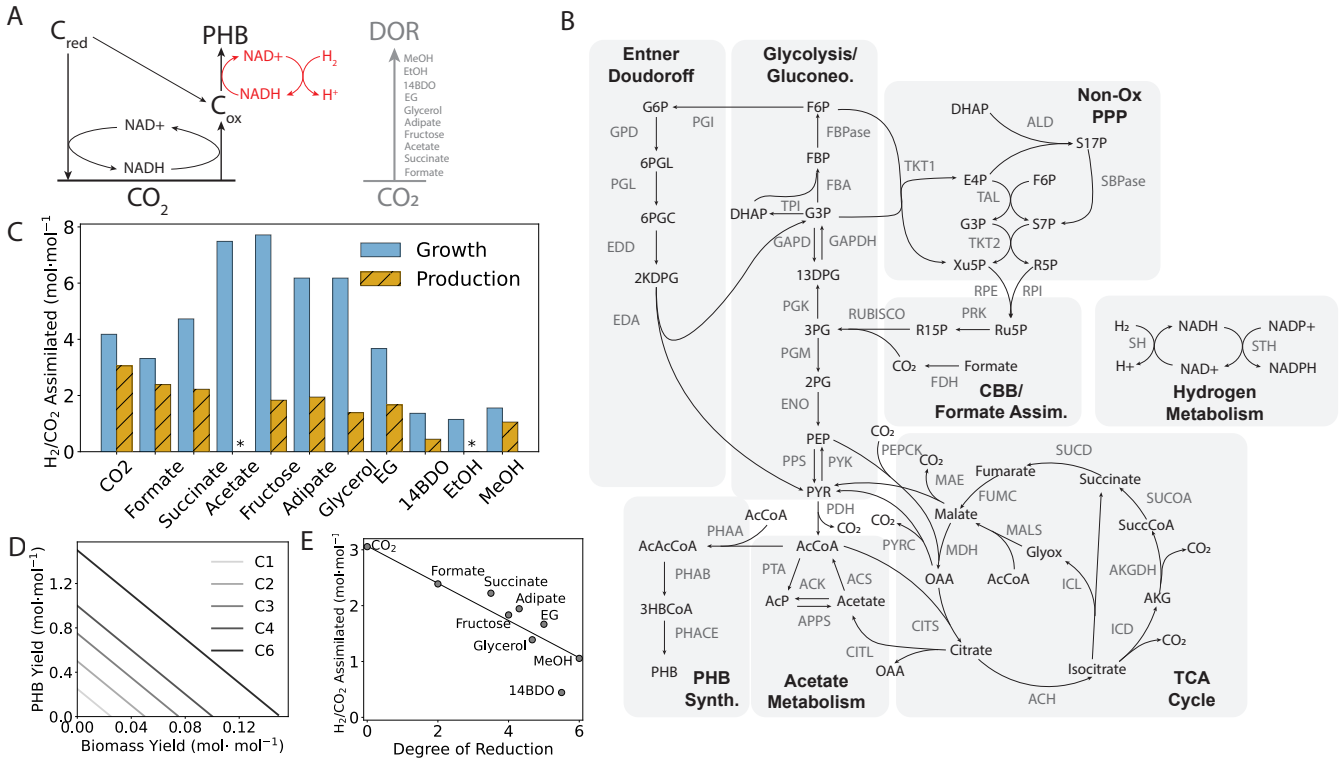

Figure 1. (A) Schematic of redox coupling using alternative, reduced substrates. Energy derived from the oxidation of reduced carbon sources (C_{red}) could be coupled to CO_2 reassimilation in *C. necator*, with additional energy for transformation to the product polyhydroxybutyrate (PHB) provided by hydrogen oxidation (shown in red). Partial oxidation of high DOR substrates may yield intermediates (C_{ox}) for PHB production. Carbon sources with a higher DOR can produce more reducing equivalents for carbon reassimilation, reducing the H_2 cost to achieve carbon conservation. (B) Map of the core metabolic model used in this work. This model was adapted from [33] with the addition of a soluble hydrogenase (SH) that can harvest reducing equivalents from H_2. The model has 79 reactions and 68 species. CBB: Calvin-Benson-Bassham cycle; STH: soluble transhydrogenase. See Supplemental Material for complete metabolite and reaction coding. (C) Hydrogen cost per assimilated molecule of CO_2 for growth-only and PHB production-only modes for all carbon sources investigated. All CO_2 generated via substrate oxidation was forced to be reassimilated with required reducing equivalents provided by H_2 oxidation. Asterisks indicate carbon sources for which no CO_2 reassimilation is required for production. (D) Production envelopes for carbon conservative fermentation. For all carbon sources, forced reassimilation of CO_2 results in stoichiometric conversion (see Fig. S1B), so production envelopes depend only on carbon number (Cn). (E) H_2 cost as a function of DOR for all carbon sources. A line is drawn to show the expected H_2 cost if all carbon were fully oxidized to CO_2 then reassimilated. Carbon sources falling above the line require more H_2 than this to achieve carbon conservation.

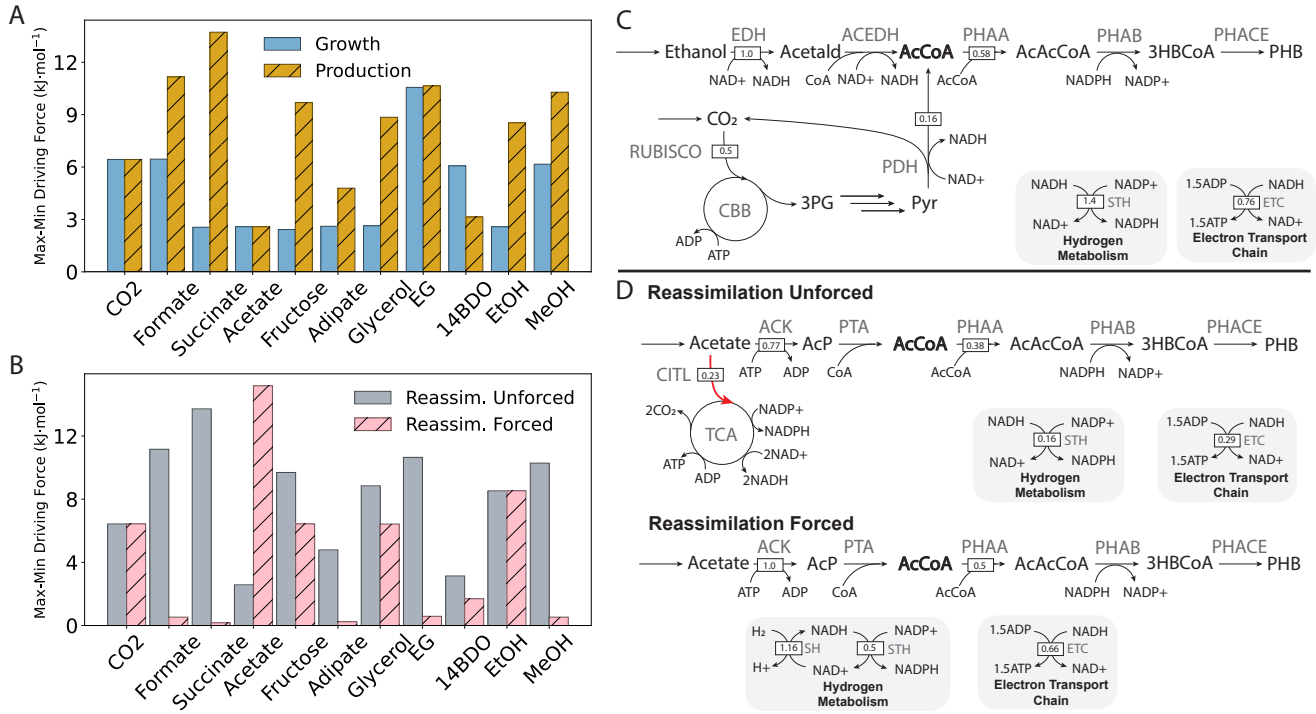

Figure 2. (A) Maximum-minimum thermodynamic driving force (MDF) for each carbon source for growth-only and production-only extremes with carbon loss (i.e. CO_2 excretion) allowed. For all carbon sources except CO_2, H_2 exchange was blocked so that energy and carbon could be derived only from the given carbon source. Positive MDFs - required for thermodynamic feasibility - are possible for all carbon sources, but MDFs are dependent on RuBisCO flux constraints (see Fig. S2). (B) MDF comparison for forced carbon conservation ('Reassim. Forced') and non-conservative ('Reassim. Unforced') PHB production. In the carbon conservative case, CO_2 excretion was blocked and H_2 exchange was unconstrained, as in Fig. 1A. For all carbon sources other than acetate and ethanol, forced reassimilation is practically thermodynamically infeasible relative to CO_2 excretion. (C) Flux map for ethanol transformation to PHB with relative flux indicated. Ethanol does not require H_2 for carbon conservative production, because its oxidation produces acetyl-CoA, which directly feeds into the PHB pathway, as well as excess reducing equivalents. The CBB cycle actively reduces CO_2 to balance redox when ethanol is the substrate for PHB production. EDH: ethanol dehydrogenase; ACEDH: acetaldehyde dehydrogenase; PHAA: acetoacetyl-CoA ; PHAB: (R)-3-Hydroxybutanoyl-CoA:NADP+ oxidoreductase; PHACE: PHB synthase; acetald: acetaldehyde; AcCoA: acetyl-CoA; AcAcCoA: acetoacetyl-CoA; 3HBCoA: (R)-3-hydroxybutyryl-CoA (D) Flux maps for acetate transformation to PHB with CO_2 reassimilation unforced (top panel) and forced (bottom panel) with relative flux indicated. In the unforced scenario, 23% of assimilated acetate must be converted to reducing equivalents via the CO_2-producing TCA cycle. Citrate lyase (CITL) activity (shown in red) is required for energy production. CITL is the thermodynamic bottleneck in this scenario, as it operates at the MDF of 2.58 kJ·mol^{-1}. In the forced reassimilation scenario, H_2 oxidation provides sufficient reducing power for all of the assimilated acetate to be converted to PHB with no CO_2 generation, and therefore no reassimilation required. ACK: acetate kinase; PTA: phosphotransacetylase.

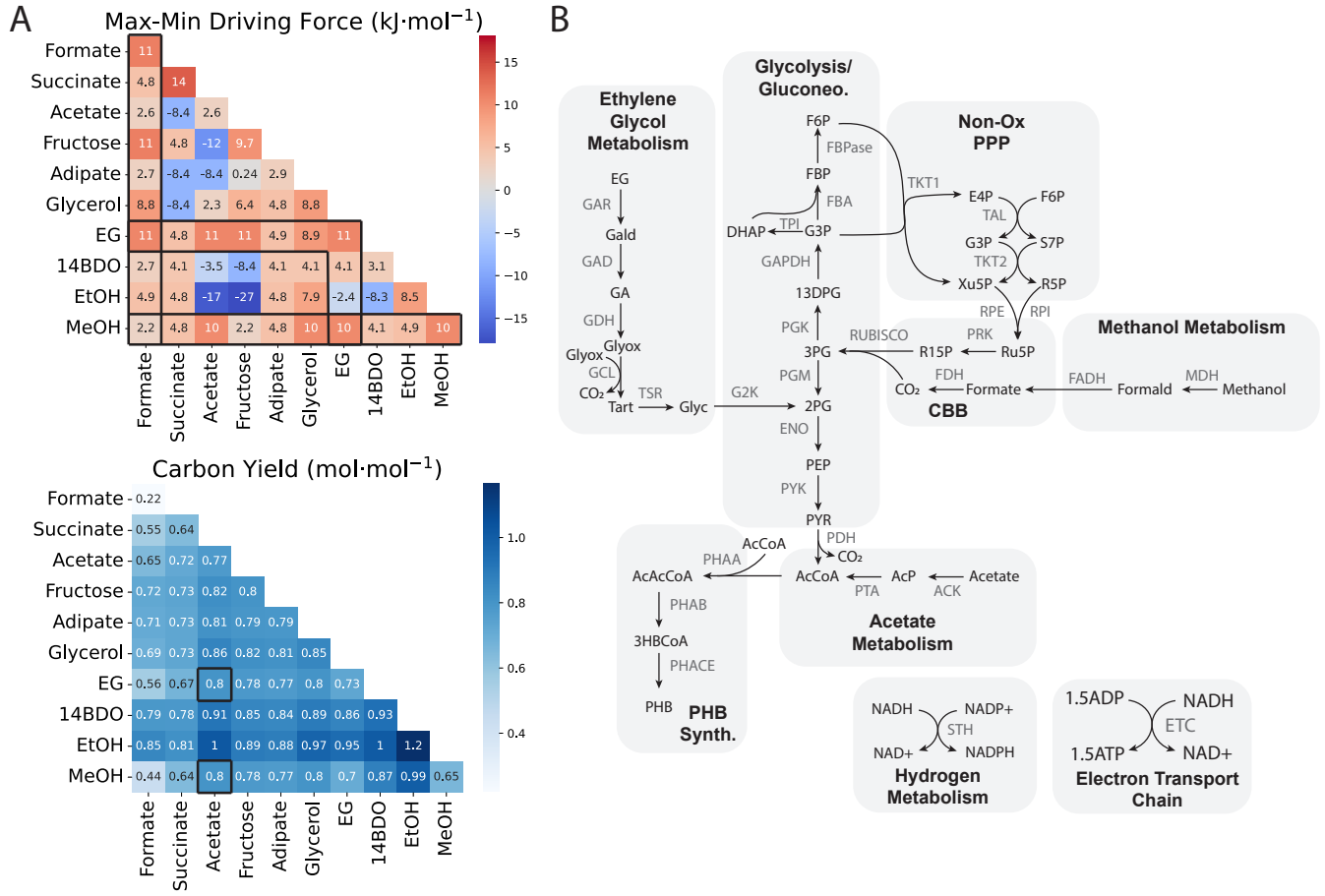

Figure 3. (A) Mixotrophic performance for all possible carbon source pairings. MDFs for all pairings are in the top panel, while carbon yields (carbon in PHB per total carbon provided) for the same are in the bottom panel. Both matrices are symmetrical, so only the lower triangle is shown. Sole carbon source scenarios are along the diagonals. Carbon sources with thermodynamically viable pairings are boxed; these include formate, ethylene glycol (EG), and methanol (MeOH). Thermodynamically viable pairings with increased carbon yields relative to the corresponding single carbon source scenarios are boxed in the lower panel. Just two pairings (EG-acetate, MeOH-acetate) are both thermodynamically viable and result in improved carbon yields. (B) Flux map for the two viable mixotrophies. Relative fluxes are not shown, but active reactions and their directions are. See Figs. S3 and S4 for relative fluxes. EG enters central carbon metabolism via 2-phosphoglycerate (2PG) following a multi-step oxidation pathway, while methanol enters via formate after two oxidation reactions. Both assimilation pathways yield sufficient reducing power such that acetate can be directly converted to PHB without any carbon loss for energy generation. Excess reducing equivalents drive incomplete, but thermodynamically feasible CO_2 reassimilation via the CBB cycle, resulting in improved carbon efficiency compared to that of EG, MeOH, or acetate as sole carbon sources. GAR: glycoaldehyde reductase; GAD: glycoaldehyde dehydrogenase; GDH: glycolate dehydrogenase; GLC: glyoxylate carboligase; TSR: tartonate semialdehyde reductase; G2K: glycerate-2-kinase; Gald: glycoaldehyde; GA: glycolic acid; Glyox: glyoxylate; Tart: tatronate semialdehyde; Glyc: glycerate; MDH: methanol dehydrogenase; FADH: formaldehyde dehydrogenase; Formald: formaldehyde

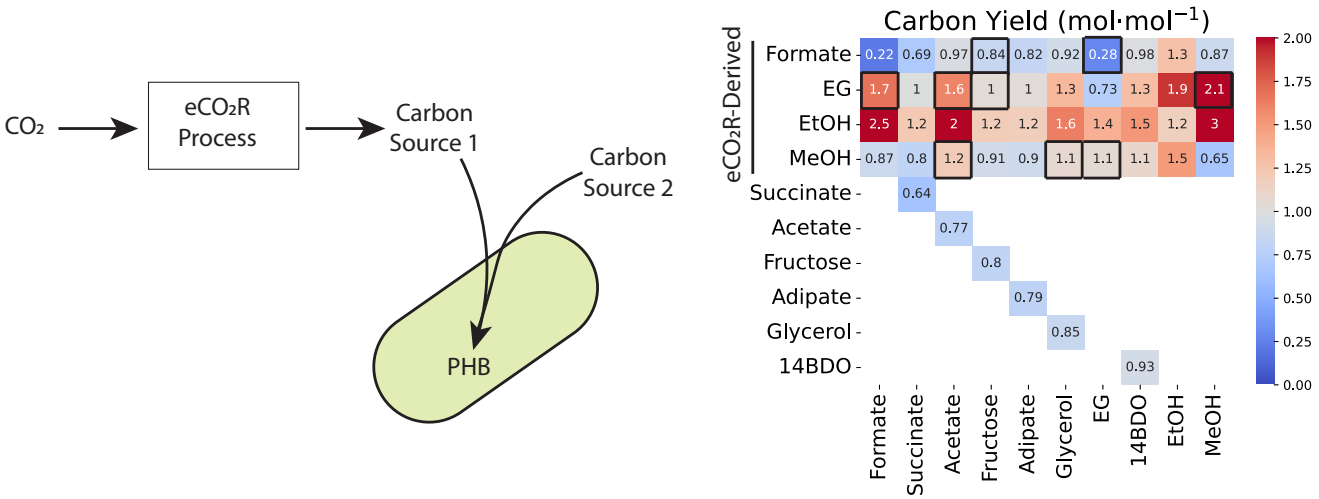

Figure 4. Carbon yield for mixotrophies with one co-substrate derived from a CO_2-free eCO_2R process. In this hypothetical scenario, CO_2 is converted to Formate, EG, EtOH, or MeOH, which is then co-fed to a mixotrophic strain with another sustainably-derived feedstock. In the ideal case, carbon from the eCO_2R-derived co-substrate does not factor into the carbon yield. Yields for thermodynamically feasible pairings with one co-substrate being eCO_2R-derived are boxed. CO_2-free EG would provide the largest feasible increase to carbon yield, possibly resulting CO_2-negative conversion of its co-substrates. Yields for sole consumption scenarios are included for comparison.

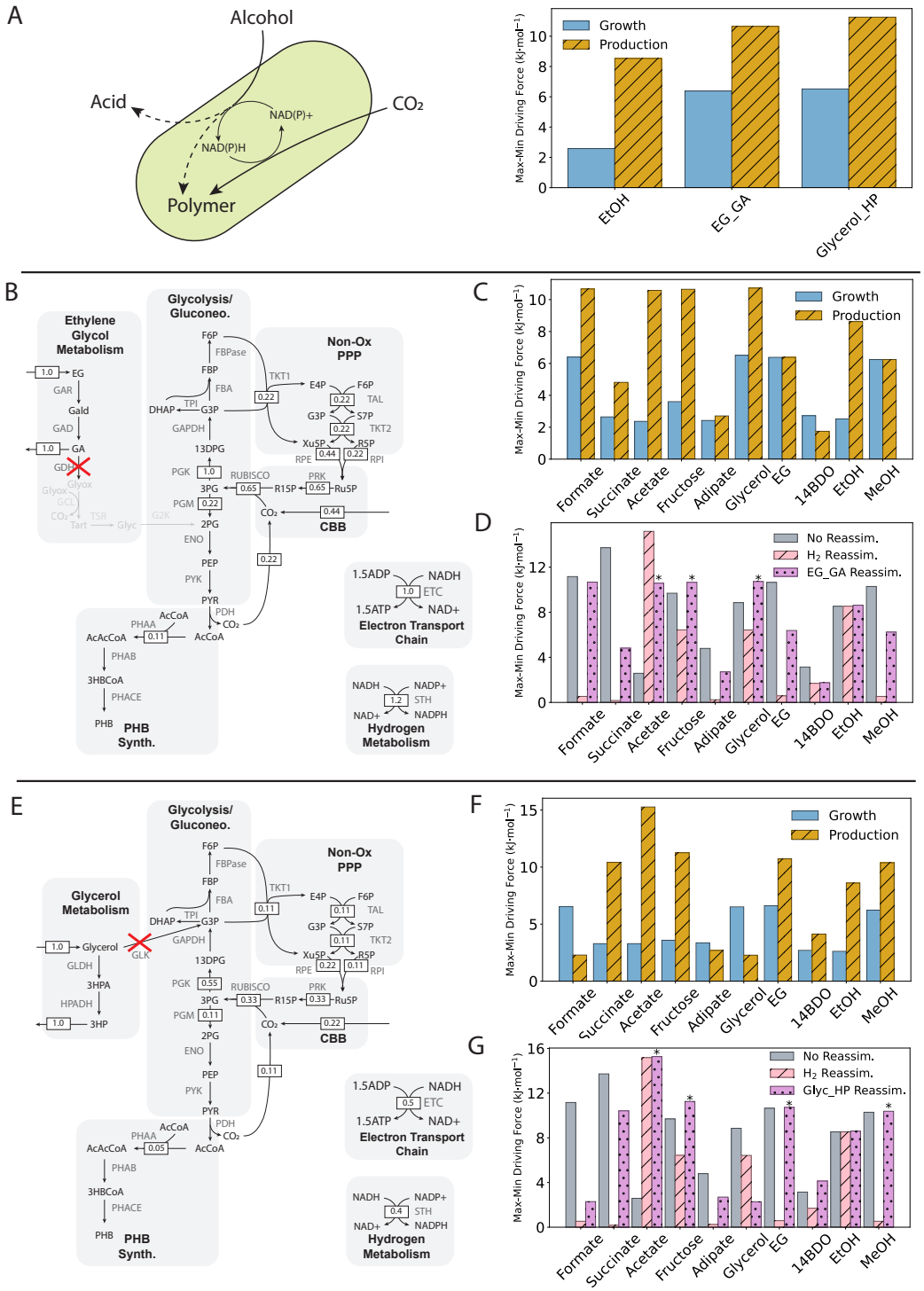

Figure 5. (Contd.)

Figure 5. (A) Alcohols as CO_2-free, carbon-based electron sources. The partial oxidation of alcohols to exported value-added acids, or biosynthetic intermediates can provide excess reducing equivalents in place of H_2, with concomitant CO_2 reduction to a biopolymer, such as PHB. Of all carbon sources examined, only ethanol, EG with glycolic acid (GA) export ('EG_GA'), and glycerol with 3-hydroxypropionate (3HP) export ('Glycerol_HP') can feasibly support growth and production without an additional electron source. Oxidation of the alcohol generates sufficient reducing equivalents for CO_2 conversion to biomass or PHB. (B) Flux map for EG partial oxidation with relative fluxes indicated. Glycolyate dehydrogenase (GDH) activity must be blocked to prevent EG assimilation into central carbon metabolism. The oxidation of a single mole of EG to GA yields sufficient reducing equivalents to drive the transformation of 0.44 moles of CO_2, resulting in 0.11 molecules of PHB, alongside 1 mole of GA. (C) Thermodynamic feasibility of mixotrophy with EG as a source of electrons. For all carbon sources investigated, mixotrophic fermentation is thermodynamically feasible for both growth-only and PHB production-only modes. (D) Thermodynamic feasibility of various reassimilation scenarios. EG partial oxidation is only a viable mixotrophic strategy if the MDF is higher than the case in which CO_2 is excreted ('No Reassim.'). Asterisks indicate co-substrates for which this is the case: acetate, fructose, and glycerol. In general, EG-supported reassimilation is more thermodynamically favourable than H_2-supported reassimilation ('H_2 Reassim.'), except in the case of acetate mixotrophy. (E) Flux map for glycerol partial oxidation with relative fluxes indicated. Glycerol kinase (GLK) activity must be blocked to prevent glycerol assimilation into central carbon metabolism. The oxidation of a single mole of glycerol to 3HP yields sufficient reducing equivalents to drive the transformation of 0.22 moles of CO_2, resulting in 0.05 moles of PHB produced, alongside 1 mole of 3HP. (F) Thermodynamic feasibility of mixotrophy with glycerol as a source of electrons. For all carbon sources investigated, mixotrophic fermentation is thermodynamically feasible for both growth-only and PHB production-only modes. (G) Thermodynamic feasibility of various reassimilation scenarios. Glycerol partial oxidation is a viable mixotrophic strategy for acetate, fructose, glycerol, and methanol (MeOH). Glycerol-supported reassimilation is more thermodynamically favourable than H_2-supported reassimilation ('H_2 Reassim.') for all co-substrates